Anal. Methods Environ. Chem. J. 6 (4) (2023) 76-92

AMECJ

Research Article, Issue 4
Analytical Methods in Environmental Chemistry Journal
Journal home page: www.amecj.com/ir

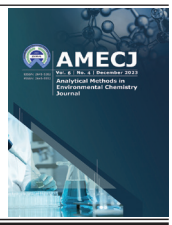

Removal of manganese (II) in water samples by the aeration-filtration process and determination based on 5-Br-PADAP ligand by cathodic stripping voltammetry

Abdoulkadri Ayouba Mahamane*[a,b,c], Boubié Guel[b], and Paul-Louis Fabre[c]

[a] *Materials, Water, Environment Laboratory, Faculty of Sciences and Techniques/University Abdou Moumouni, BP 10662, Niamey - Niger*

[b] *Laboratory of Materials and Molecular Chemistry, U.F.R –SEA/University Joseph Ki-ZERBO, Ouagadougou 03 BP 7021, Burkina Faso*

[c] *Chemical Engineering Laboratory UMR CNRS 5503 Bât.2R118 – 1 route de Narbonne 31062 Toulouse Cedex09, France*

ARTICLE INFO:

Received 7 Aug 2023
Revised form 24 Oct 2023
Accepted 27 Nov 2023
Available online 28 Dec 2023

Keywords:
Manganese,
Removal,
5-Br-PADAP Ligand,
Aeration-filtration,
Cathodic Stripping Voltammetry,

ABSTRACT

In this study, manganese (Mn II) was determined in aqueous media by an electrochemical method, and its removal was evaluated using the aeration-filtration process (AFP). An electrochemical sensor based on carbon paste (EPC) modified with the 5-Br-PADAP ligand was used to measure Mn (II) in aqueous media. Through the optimization of analytical parameters in cathodic stripping voltammetry (CSV), real boreholes and well water samples could be analyzed for manganese content. The optimum parameters such as preconcentration potential (1100 mV), preconcentration time (240s), 5-Br-PADAP ligand concentration (20 µmol L^{-1}), and electrode rotation speed during pre-concentration (1000 rpm) were studied and optimized. The detection limit (LOD) is estimated at 3 $\times 10^{-7}$ mol L^{-1} with a relative standard deviation (RSD) of 3.36%. The real samples showed that some water points have more concentration than the standard. A simple, effective, inexpensive, and rural-friendly method was used for treating manganese-rich water. Following the aeration phase, the sand and gravel column was filtered to remove manganese (II) from the water. The removal efficiency of Mn was obtained at a rate of 74.8- 84.5% and more than 95% after two hours of aeration and 1 hour at pH 8 for real samples.

1. Introduction

Manganese is a trace element in the environment. Besides being essential for human growth, it also plays an important role in carbohydrate and lipid metabolism and catalyzes certain enzymatic reactions [1]. Due to its antagonistic nature towards calcium, it may also cause irreversible neurological disorders. These disorders generally occur when manganese levels exceed 2 mg L^{-1} [2]. Manganese is mainly found in ores such as pyrolusite (MnO_2) and rhodochrosite ($MnCO_3$). It is widely used in metallurgy (steels, alloys, welds), the electrical industry (electrodes, dry cells), the chemical industry (catalysts, colorants), the glass and ceramic industries, and in fuel production (organometallic additives). Depending on pH, dissolved oxygen, and complexing agents, manganese is found in water in different valences (II, III, and IV), soluble or suspended forms, or complexes. Occasionally,

*Corresponding Author: Abdoulkadri Ayouba Mahamane
Email: kadayouba@gmail.com
https://doi.org/10.24200/amecj.v6.i04.313

groundwater contains a level of 1 mg L^{-1}, especially when attacked by water from the support rock in a reducing environment or when certain bacteria are active. Under these conditions, it is often associated with iron, with which it co-precipitates by oxidation. Generally, surface waters contain less than 0.05 mg L^{-1} [1]. Manganese can give water an unpleasant taste. Furthermore, even at the lowest dose (0.02 mg L^{-1}), it can form a black layer (on pipes), making the water unattractive when detached. Even small quantities (0.1 mg L^{-1}) can stain enamel and linen, which is a problem from a domestic standpoint. As a result, it stimulates the growth of siderobacteria (Galllionella) in water treatment plants, disrupting the operation of sand filters and resulting in pipe deposits. It can, however, be used in its heptavalent state as permanganate to eliminate organic matter, giving water an unpleasant taste. The WHO recommends a provisional guideline value of 0.4 mg L^{-1} for water intended for human consumption [1, 3]. Various analytical methods have been used to analyze manganese. The two most used methods are flame atomic absorption spectrometry (F-AAS) and UV-visible spectrophotometer [4]. Implementing these methods is time-consuming, requiring long sample time and pretreatment of samples before determining the element content of the matrix under study [5]. Electrochemical methods are an appealing alternative for detecting manganese traces due to their rapidity, high sensitivity, and selectivity. These methods have the advantage of working with a small sample quantity and without pretreatment of the sample [5]. Anodic stripping voltammetry (ASV) with mercury drop or mercury film electrodes is the most widely used method for determining trace metal concentrations in electrochemistry [6, 7]. Since manganese is poorly soluble in mercury and requires a high overpotential to be deposited on mercury, this method presents some analytical challenges for manganese determination [8]. The potential of the peak associated with manganese deposition on the mercury electrode and the potential of the hydrogen reduction wave are close. Further, manganese determination is difficult due to intermetallic compounds formed with copper [5]. All these factors considerably reduce the sensitivity of the method. Several alternatives have been described in the literature as solutions to these difficulties. Several solid electrodes (graphite, glassy carbon, carbon fiber, platinum, boron-doped diamond, etc.) have been used to measure manganese traces through cathodic stripping voltammetry (CSV) [9, 10] after oxidized Mn (II) to MnO_2 [11]. In addition, it is possible to perform voltammetry using a manganese complex adsorbed on the surface of a mercury or solid electrode after the complex has been pre-concentrated on the electrode surface. Several researchers have used cathodic stripping voltammetry (CSV) of an adsorbed complex to determine various inorganic cations, including metals that do not form amalgams with mercury. As a result, metals such as Fe, Mn, Ni, Co, Al, Se, As, and Ti have been determined in natural waters after complexation of the ligands cation (such as dimethylglyoxime, catechol or oxine), which is followed by adsorption and cathodic stripping. The CSV technique has achieved detection limits of 10^{-12} M [12]. Azo compounds are compounds with the functional group R-N=N-R' in their structure. The 2-(5'-Bromo-2'-pyridylazo)-5-diethylaminophenol group (5-Br-PADAP) is an azo compound used as a ligand capable of forming complexes with several metal ions. Cathodic stripping voltammetry (CSV) has successfully been used to determine several metal cations, including Mn (II), Cu (II), Fe (III), V(V), Bi (III), Cr (III), Co (II), and Ti (IV) [13, 14]. In this paper, cathodic stripping voltammetry is used for electrochemically determining manganese (II) based on the work of E. Ghoneim *et al.* [13]. Numerous studies have examined manganese removal from water [15-17]. Processes commonly used include chemical oxidation with chlorine derivatives, ozone or permanganate, and biological methods. While it produces good yields, these processes are not feasible in rural areas because of their high cost and toxicity [2]. In this article, the

first objective is to develop an electrochemical sensor for manganese (II) determination using 2-(5'-bromo-2'-pyridylazo)-5-diethylaminophenol (5-Br-PADAP) ligand-modified carbon paste. In an aqueous matrix, optimal analytical parameters are established for the electrochemical determination of manganese. As part of a real-life evaluation of the electrochemical sensor, manganese pollution in boreholes and well waters were investigated near Ouagadougou (Burkina Faso). Considering manganese pollution in rural areas of developing countries, the second objective of this article is to propose a simple method for removing manganese from water.

2. Experimental

2.1. Chemicals and solutions

Ultrapure water (milli-Q water) was used for all solutions. Mn^{2+} (10^{-3} mol L^{-1}) solution was prepared by dissolving manganese sulphate (purity > 99.99%, Sigma Aldrich, CAS N.: 10034-96-5) in 0.1 M perchloric acid (trace analysis, Sigma Aldrich, CAS N.: 7601-90-3). A certified manganese standard (1.0 g L^{-1}) (Certipur Merck, CRM 119789) was also used to prepare standard solutions. The supporting electrolyte was a 0.1 mol L^{-1} acetate buffer (pH 4.5) prepared with acetic acid (Normapur ACS 95%, VWR, CAS N.: 64-19-7) and sodium acetate (99.5%, Sigma Aldrich, CAS N.: 127-09-3). The ligand used to complex Mn^{2+} ions is 2-(5'-Bromo-2'-pyridylazo)-5-diethylaminophenol (5-Br-PADAP, 97% Sigma Aldrich, CAS N.: 14337-53-2). 5-Br-PADAP solution is obtained by dissolving the appropriate quantity in pure methanol (99.8% Sigma Aldrich, CAS N.: 67-56-1).

2.2. Carbon paste electrode preparation

The carbon paste electrode used was made by mixing 2.0 g of graphite powder (diameter < 0.1 mm, 99.9995% Alfa Aesar, CAS N.: 7782-42-5) and 0.72 mL paraffin oil (Sigma Aldrich, CAS N.: 8012-95-1) in an agate mortar until a homogeneous paste was obtained. The paste is manually inserted into the cylindrical cavity of the rotating disk electrode's cylindrical tip. The surface of the tip is then smoothed on clean paper.

2.3. Apparatus

The experimental set-up used for DPCSV (Differential Pulse Cathodic Stripping Voltammetry) and Cyclic Voltammetry (CV) analyses is a PGstat potentiostat-galvanostat model Voltalab 50 (Radiometer, Copenhagen) controlled by a microcomputer running Volta Master software (version 4.0). The dropping mercury electrode (DME) 150 measuring stand comprises a cell (25 mL) containing an EDI 101 rotating disk electrode with carbon paste tip (diameter 3 mm), a silver chloride, Ag/AgCl, 3 mol L^{-1} KCl reference electrode (E_{ref}=0.205 V/ENH. Also, radiometer model TR020), a platinum auxiliary electrode (Radiometer model TM020) and a nitrogen supply for solution bubbling were used. The morphology and chemical composition of the surface-adsorbed complex were obtained using a scanning electron microscope (SEM controlled by a microcomputer running TM-100 software, Hitachi, Japan) coupled to an EDX system (Swift ED-TM software) for chemical analysis of the electrode surfaces.

2.4. Analytical procedure for manganese (II) analysis

The three electrodes are immersed in the electrochemical cell containing the electrolyte. During the study of the ligand alone, the supporting electrolyte consists of 10 mL of acetate buffer solution and 20 µmol L^{-1} of 5-Br-PADAP (10^{-3} mol L^{-1}). For the analysis of the Mn (II)-(5-Br-PADAP) complex, the supporting electrolyte contains 5.0 mL of acetate buffer solution, 20 µmol L^{-1} of 5-Br-PADAP (0.001 M) and 5 mL of the Mn^{2+} ion solution were used. An anodic pre-concentration potential is applied to the electrode under constant rotation of 1000 rpm. The differential pulse cathodic stripping voltammetry is used for recording the voltammogram after 10 seconds of pre-concentration (Fig. 1). A simple standard addition method is used to determine the exact concentration of Mn^{2+} ions in the borehole and well waters.

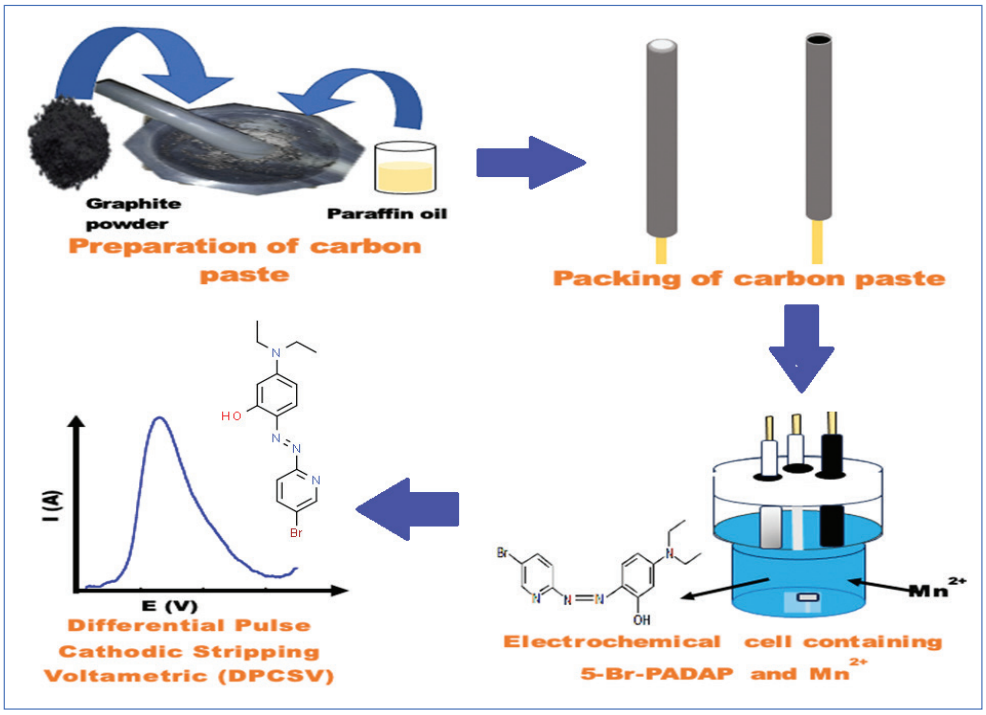

Fig. 1. Schema of analytical procedure

2.5. Real samples of borehole and well waters

The present method is applied to the determination of Mn^{2+} in the borehole and well waters from the locality of Yamtenga, south-east of the city of Ouagadougou, with UTM coordinates: X = 669126, Y = 1363944. Samples were taken at 11 water points (9 boreholes and two wells) every three months for one year.

2.6. Raw materials for manganese (II) removal

Sand samples were collected in the southern part of the town of Bobo-Dioulasso in Burkina Faso from a sand zone extensively exploited by residents. Three (03) sand samples were collected from different sites in this area. In the text, they were referenced to facilitate their identification. Table 1 summarizes the references for the sand samples and the sampling locations. The S_1 and S_3 samples belong to the *Kawara-Sindou* formation, while the S_2 sample belongs to the *Tabalédougou* formation. These geological formations comprise fine, very fine, or coarse sandstone-quartzite. The gravel sample was collected in the commune of Gomboussougou, in the Zoundweogo province of the Center Sud region of Burkina Faso (Table 1). The gravel sample was found in a waterway formed by erosion of alkaline granite. Alkaline granite, clear to mesocratic, has a medium to coarse-grained texture, whether porphyritic or not. In addition to the presence of alkali feldspars and quartz, this rock is also characterized by the presence of alkaline (sodic) ferromagnesian minerals.

2.7. Granulometric characterization of raw materials

Studying a sample's particle size enables us to determine the distribution of grain sizes. One of the

Table 1. Reference names of sand and gravel samples and their geographical coordinates

Sample	Characteristics	GPS coordinates (UTM)	
		X	Y
S_1	Red-brown sand	970 368	946 233 1
S_2	Pink sand	091 369	360 234 1
S_3	White sand (coarse-grained)	373 369	557 234 1
GOM	Fine gravel	633 739	074 246 1

most common methods of determining grain size is to sieve through sieves with decreasing cross-sections. It allows us to distinguish between the "pass," or quantity of product that passes through the mesh, and the "reject," or quantity that remains in the sieve. The sum of pass and reject for a given sieve equals the total sum of the product tested [18]. To determine the particle size of sand, three samples were analyzed. After washing and drying, a 100 g sample was sieved through 7 AFNOR standardized sieves. The mesh sizes in mm are 1, 0.5, 0.4, 0.35, 0.25, 0.20, 0.16, and 0.125. The calculation of the weight percentage of each refusal and that of each pass are given by Equations 1 and 2 [2].

$$\% \text{ Rejection} = (A/B)\times 100 \quad \text{(Eq. 1)}$$

$$\% \text{ Passing} = ((B-A)/B)\times 100 \quad \text{(Eq. 2)}$$

With: A, weight of refused material in g and B, initial weight.

These percentages are used to establish the granulometric curve of the sand samples and determine the Coefficient of Uniformity (CU) as Equation 3.

$$CU = d_{60}/d_{10} = d_{40}/d_{90} \quad \text{(Eq. 3)}$$

Where d_{60} (d_{40}) is the diameter through which 60% of the sand passes (retaining 40% of the sand) and d_{10} (d_{90}) is the diameter through which 10% of the sand passes (including 90% of the sand).

Knowing the CU lets us know whether the sand is homogeneous and, therefore, suitable for filtration. Homogeneity is achieved if $1.2 \leq CU \leq 1.8$ [2]. The diameter through which 10% of the sand can pass is called the effective size, $ES = d_{10}$ [19]. Gravel particle size analysis was also carried out according to the abovementioned procedure. AFNOR standard sieves have mm dimensions (6, 4, 3.15, 2.5, 2, 1.6, 1.25, 1).

2.8. Filter description and analytical procedure for removal tests

To implement the method of aeration followed by filtration, we carried out laboratory-scale tests using a filtration column. The column is shown in Figure 2, with the following characteristics: length 43 cm, outside diameter 4 cm, and inside diameter 3.2 cm. The column is filled with a 10 cm layer of gravel, topped with 20 cm of sand. The sand and gravel are washed thoroughly with water to remove any impurities that may contaminate the treated water. For the manganese removal tests, we intentionally spiked ultrapure water with Mn (II) at 5 mg L^{-1} (an arbitrary concentration corresponding to water with

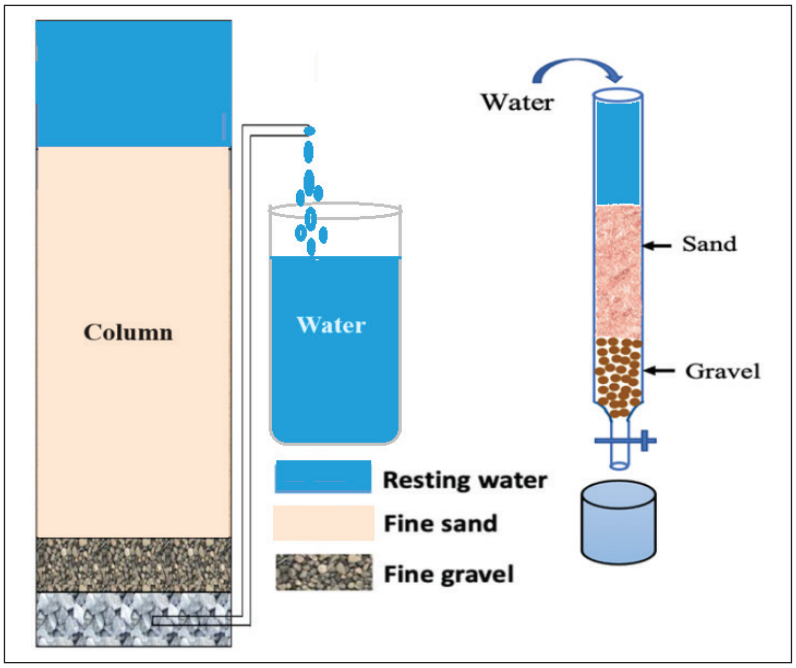

Fig. 2. Filtration column for aeration-filtration

a high Mn (II) content). This water was aerated with atmospheric oxygen for a total of 120 min. The water was passed through the column at time intervals, and the residual Mn (II) concentration was determined. The analysis was conducted at three different pH levels (6, 7, and 8). These three pH values generally cover the pH of groundwater. Concentrated NaOH sodium hydroxide and HCl hydrochloric acid were used to adjust the pH of the water. The method for determining Mn^{2+} ions is described in section 2.4.

3. Results and discussion

3.1. Voltammetric determination of manganese (II)

3.1.1. Cyclic and differential pulse voltammetry

Figure 3a shows the voltammogram recorded in a solution of the supporting electrolyte containing only Mn^{2+} ions. Due to the Results, no anodic or cathodic peaks are recorded with or without pre-concentration potential. Based on the contact of Mn^{2+} ions with the ligand, the voltammogram is shown in Figure 3b. Also, a cathodic sweep from 1.1 V to 0.4 V was performed without pre-concentration potential by a return sweep. In Figure 3b, we obtain an anodic signal, at 0.80 V, but no significant signal exists in the cathodic direction. After pre-concentration at a potential of +1.1 V for 2 min under constant electrode rotation, we record cyclic voltammetry, a cathodic peak at 0.644 V, in addition to an intense anodic peak at 0.84 V (Fig. 3c). The increase in ligand and manganese concentration also leads to an increase in the intensities of the two peaks and. The difference ΔE between the potentials of the anodic and cathodic peaks in the voltammogram of Figure 3c is equal to 0.22 V, reflecting the high degree of irreversibility of the processes involved [20]. In DPCSV, as expected, we obtain an intense, better-resolved cathodic peak (Fig. 4). DPCSV will be used to analyze manganese in wells and boreholes water. Consequently, the accumulation process

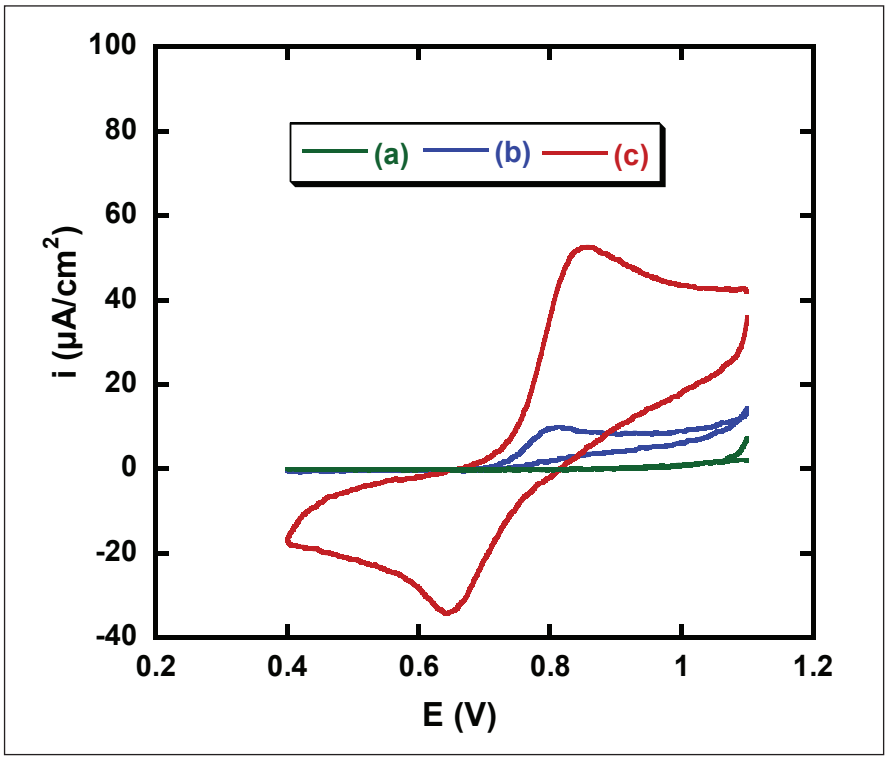

Fig. 3. Cyclic voltammograms at the carbon paste electrode at 25 mV/s: (**a**) in the supporting electrolyte (acetate buffer 0.1 mol.L^{-1} pH 4.5) containing Mn^{2+} ions 4 ×10^{-6} mol.L^{-1} with or without pre-concentration potential; (**b**) in the supporting electrolyte containing Mn^{2+} ions 4×10^{-6} mol.L^{-1} and ligand 5-Br-PADAP 20 µmol.L^{-1} without pre-concentration potential, cathodic then anodic direction (from 1.1 V to 0.4 V); **(c)** same conditions as in (b), except that a pre-concentration potential is imposed (pre-concentration potential: 1.1 V; pre-concentration time: 2 min; electrode rotation: 1000 rpm)

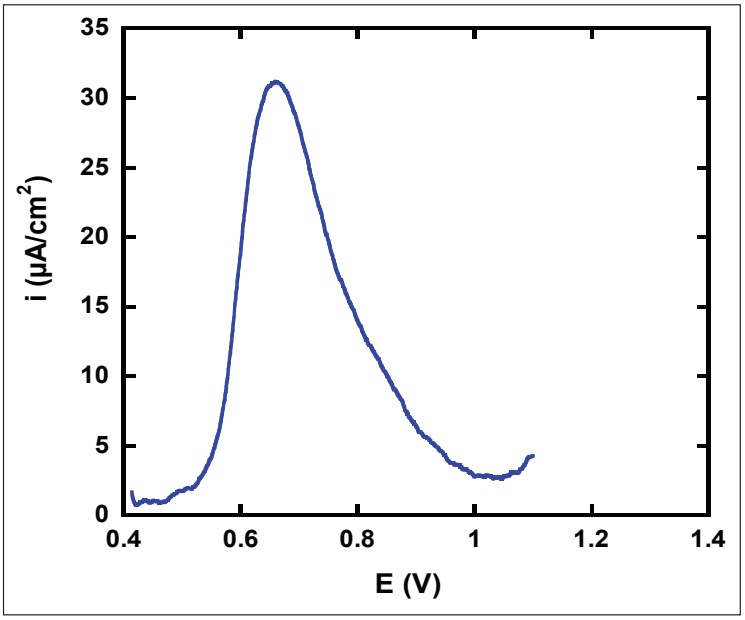

Fig. 4. DPCSV of a standard solution of Mn^{2+} ions 1.5 ×10^{-6} mol.L^{-1} in the supporting electrolyte after addition of 20 µmol.L^{-1} of the 5-Br-PADAP ligand, with pre-electrolysis before voltammogram recording (pre-concentration potential: 1.1 V; pre-concentration time: 2 min; electrode rotation: 1000 rpm)

at positive potential enhances the adsorption of the complex to the electrode surface. This is not a simple accumulation of material in the interfacial zone but a reactive phenomenon leading to specific adsorption on the electrode surface.

3.1.2. Effect of pre-concentration potential

Figure 5 illustrates the variation of peak current with pre-concentration potential. The highest peak current was obtained at a potential of 1100 mV. Therefore, this potential was chosen as the pre-concentration potential.

3.1.3. Effect of pre-concentration time

Cathodic stripping peak current was studied by varying pre-concentration time between 0 and

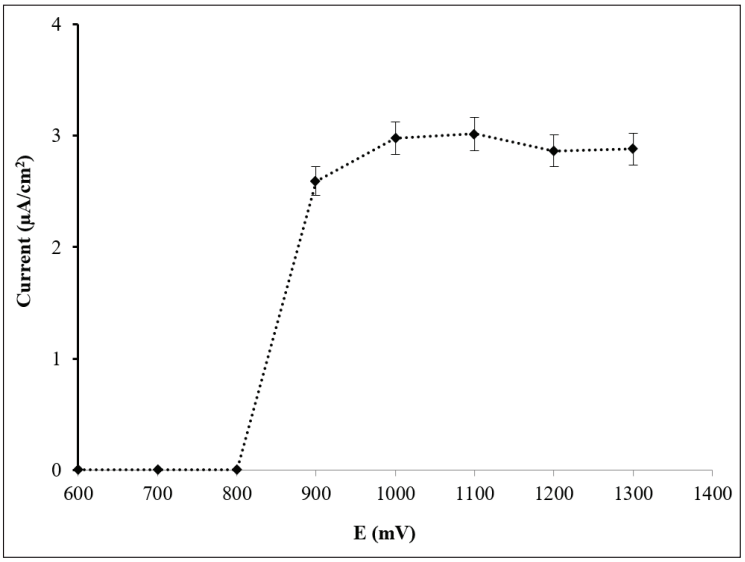

Fig. 5. Effect of pre-concentration potential on reduction peak current (pre-concentration time 2 min, rotation speed 400 rpm, 5-Br-PADAP: 50 µmol L^{-1})

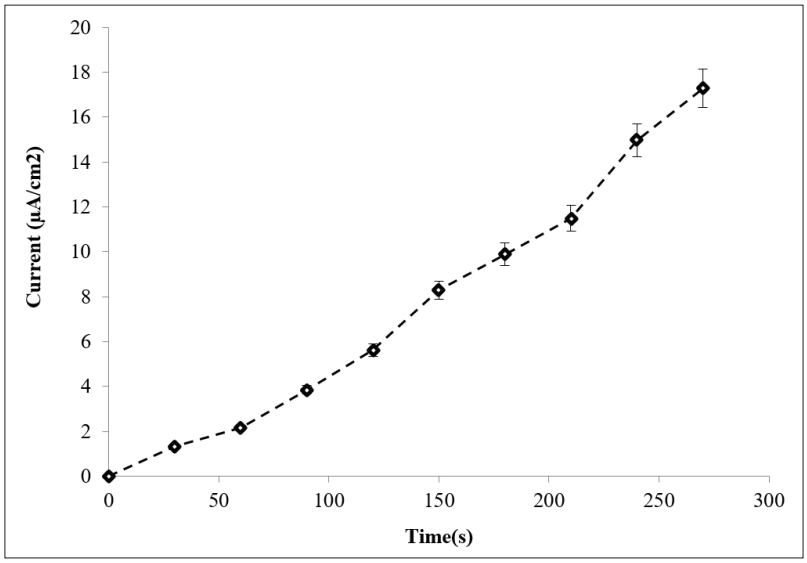

Fig. 6. Effect of pre-concentration time on reduction peak current
(pre-concentration potential 1100 mV, stirring 400 rpm, 5-Br-PADAP: 50 µmol L^{-1}, pulse amplitude 40 mV)

300 seconds. Figure 6 illustrates the increase in current with increasing deposition time. For further analysis, 240 seconds were selected as the pre-concentration time.

3.1.4.Effect of electrode rotation speed

The influence of electrode rotation speed during the pre-concentration step was studied by varying this speed between 0 and 1000 rpm. The results indicate that the redissolution current increases with the rotation speed of the electrode. For the remainder of our work, we used the highest value provided by our speed controller, i.e., 1000 rpm.

3.1.5.Effect of ligand concentration

Various concentrations of 5-Br-PADAP ligand are tested, ranging from 0 to 60 µmol L^{-1}. Figure 7 shows that the redissolution current increases with 5-Br-PADAP concentration, picking at 20 µmol L^{-1} and stabilizing. Therefore, the optimum value for this parameter is 20 µmol L^{-1}.

3.1.6. Morphological study and chemical composition of the electrode surface

The morphology and chemical composition of the

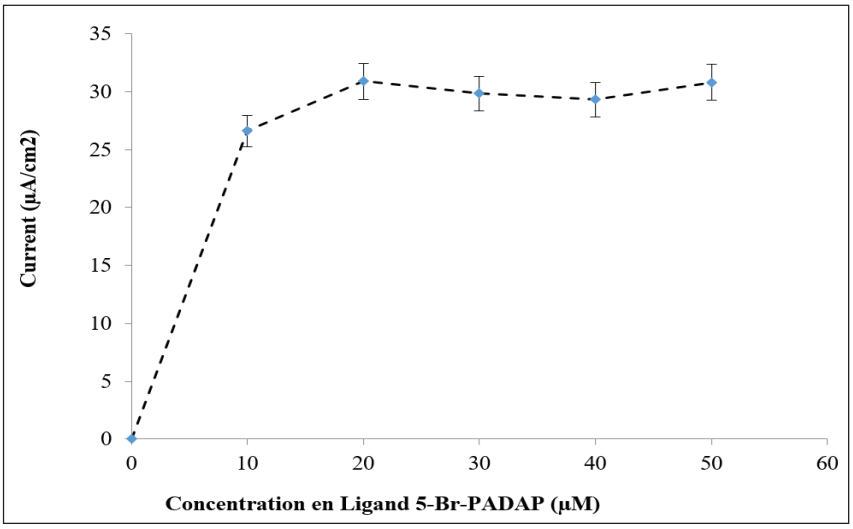

Fig. 7. Effect of 5-Br-PADAP ligand concentration on reduction peak current.
(pre-concentration potential 1100 mV, pre-electrolysis time 4 min, electrode rotation speed 1000 rpm, pulse amplitude 40 mV)

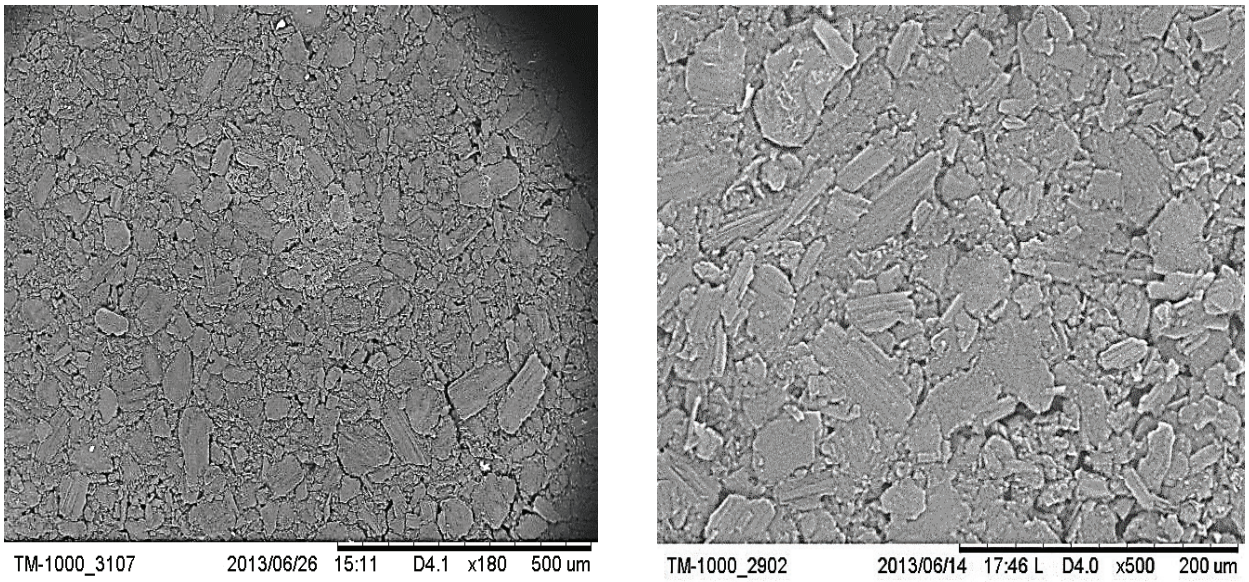

Fig. 8. SEM images at two resolutions of modified carbon paste after deposition of the manganese complex from a solution of the supporting electrolyte (acetate buffer 0.1 mol L^{-1} pH 4.5) containing the ligand 20 µmol L^{-1} and the Mn^{2+} ions 10^{-4} mol L^{-1}, the deposition potential being +1.1 V)

complex on the surface of the carbon paste electrode were established by scanning electron microscopy (SEM) combined with EDX chemical analysis. Figure 8 shows the appearance of the carbon paste electrode at a pre-concentration potential of 1.1 V carried out in a solution of the supporting electrolyte containing Mn^{2+} ions at a concentration of 10^{-4} mol L^{-1}. Different diameter plates were found assembled, identifying a chemically modified surface by a non-homogeneous complex film, i.e. a rough deposit [21]. The EDX spectrum corresponding to the image shows the presence of manganese (100% Mn and no trace of any other metal) in the layer formed on the surface at a potential of 1.1 V.

3.1.7.Analytical application

The modified electrode response towards Mn^{2+} is determined by plotting calibration curves obtained from successive additions of Mn^{2+} ions (Fig. 9). The calibration line has a correlation coefficient of 0.997, which is satisfactory for the concentration range studied. The limit of detection (LOD) is calculated as Equation 4 [22].

$$LOD = (k \times Sy)/a \quad \text{(Eq. 4)}$$

k is a constant equal to 3, Sy is the residual standard deviation between measurements, and a is the slope of the calibration line. The calculated detection limit, in the concentration range 10^{-6} – 7×10^{-6} mol L^{-1}, is 3×10^{-7} mol L^{-1} (0.016 mg L^{-1}). Then, the standard addition method assays a certified manganese standard at 1 mg L^{-1}. The recovery rate obtained was of the order of 97%. In terms of precision, the i = f(E) curve was recorded n times for a constant Mn^{2+} concentration. For n=5 and $[Mn^{2+}] = 2 \times 10^{-6}$ mol L^{-1}. A standard deviation between measurements of 0.75 was found. The calculated RSD (Relative Standard Deviation) is 3.36%.

Overall, these results are satisfactory and demonstrate that the method is reliable for determining the concentration of Mn^{2+} ions in solution. Therefore, the technique was applied

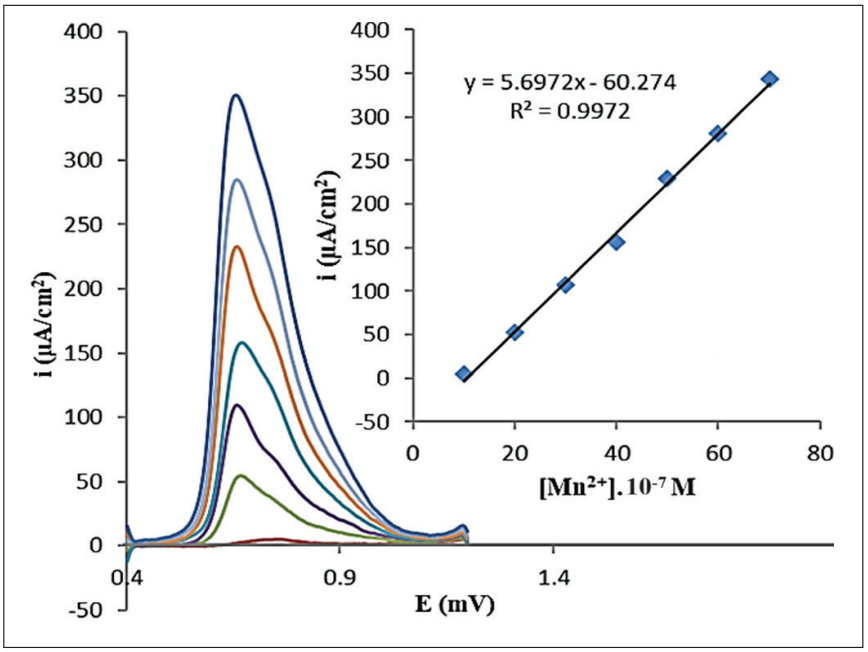

Fig. 9. Curves obtained by DPCSV after successive additions of 10 µL of Mn^{2+} ions 10^{-3} mol.L^{-1} to the supporting electrolyte solution (acetate buffer 0.1 mol L^{-1} pH 4.5) containing Mn^{2+} ions 10^{-6} mol.L^{-1}. The inset in the top right-hand corner shows the calibration line in the concentration range 10^{-6}–7×10^{-6} mol L^{-1}. (pre-concentration potential: 1.1 V; pre-concentration time: 2 min; electrode rotation: 1000 rpm)

to determine Mn^{2+} in boreholes and well water in Yamtenga. Figure 10 shows the results of measurements conducted on real samples. This figure shows the spatio-temporal evolution of manganese (II) content in this area's borehole and well water samples.

According to the analysis, manganese levels in the water ranged between 4.36 $\times10^{-3}$ and 1.738 mg.L^{-1}. Levels of these contaminants vary from one water point to another and vary according to the sampling

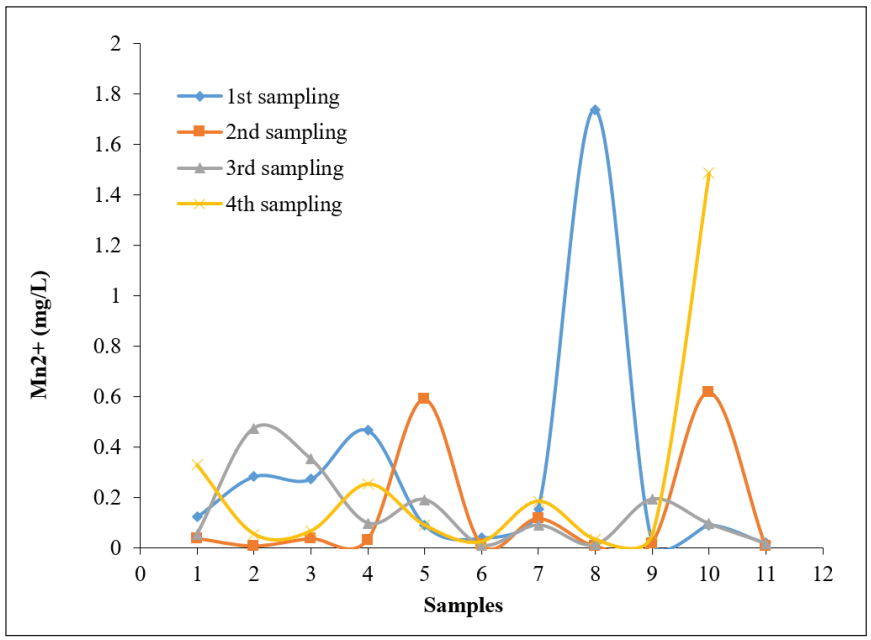

Fig. 10. Spatio-temporal evolution of manganese (II) content in real samples

period. Manganese in water is an organoleptic (metallic taste) and aesthetic nuisance (black color). Consumers can feel the nuisance at concentrations of 0.03 mg L^{-1} (the WHO standard for manganese). Waters with concentrations above the WHO standard are points 2, 4, 5, 8, and 10. As the geological landscape of the Yamtenga area consists of medium-grained gray granite with biotite and rare muscovite, manganese is not a major constituent of the granite type studied in our area, whose dissolution could result in water borehole pollution. A possible explanation for the presence of manganese in groundwater is that the manganese is infiltrated by water from the dam. Since the dam is located near a city, human activity contributes significantly to water pollution in the dam and its tributaries. Consequently, the local population rejects these water sources due to the alteration of their organoleptic characteristics, resulting in complaints about their safety.

3.1.8. Comparison to other methods

To assess the performance of the present method based on the LOD and RSD, it was compared with other methods reported in the literature for Mn (II) determination. The comparison is given in Table 2. Recently, many researchers have worked on determining manganese (II) ions in water, food, and vegetable samples using atomic absorption spectrometry, ultrasound-assisted-dispersive-micro-solid phase extraction, or multi-walled carbon nanotubes [28-31], but the proposed method based on 5-Br-PADAP coupled to DP-CSV and ASV is simple, fast, low cost and accurate/precise results as compared to others.

As a cheap instrument and a simple procedure, our electrochemical method performs relatively well at a low cost and detection limit. As a result, this sensor could be considered a good choice for Mn (II) determination.

3.2. Manganese removal by aeration-filtration

3.2.1. Granulometric analysis

The complete granulometric analysis curves for S_1, S_2, and S_3 are shown in Figure 11.

Table 2. Comparison of experimental results with reported data for Mn (II) determination

Method/ Technique	LOD	RSD	Reference
Rotating carbon paste disk electrode/DP-CSV	4×10^{-9} mol. L^{-1}	3%	[11]
Boron-doped diamond/DP-CSV	7.4×10^{-7} mol. L^{-1}	/	[23]
Bentonite–porphyrin CPE/ASV	1.07×10^{-7} mol. L^{-1}	2.30%	[24]
1-(2-pyridyl azo)− 2-naphthol – CPE/ DP-CSV	6.9×10^{-9} mol. L^{-1}	2.90 to 7.20 %	[25]
Ion-Selective Membrane Electrode/ Potentiometry	8.0×10^{-6} mol. L^{-1}	/	[26]
Silver Nanoparticles/ Colorimetry	0.06 µmol. L^{-1}	/	[27]
Immobilization on chloro-functionalized multi-walled carbon nanotubes	0.12 µg L^{-1}	/	[28]
Ultrasound assisted-dispersive-micro-solid phase extraction	0.007 µg L^{-1}	% 2.3	[29]
Flame atomic absorption spectrometry (FAAS)	0.75 µg L^{-1}	Lower than 7%	[30]
Cloud point extraction and graphite furnace atomic absorption spectrometry	0.020 (ng mL^{-1})	3.5%	[31]
CPE-5-Br-PADAP/DP-CSV	3×10^{-7} mol.L^{-1}	3.36%	This work

DP-CSV: differential pulse cathodic stripping voltammetry
ASV: Anodic Stripping Voltammetry.

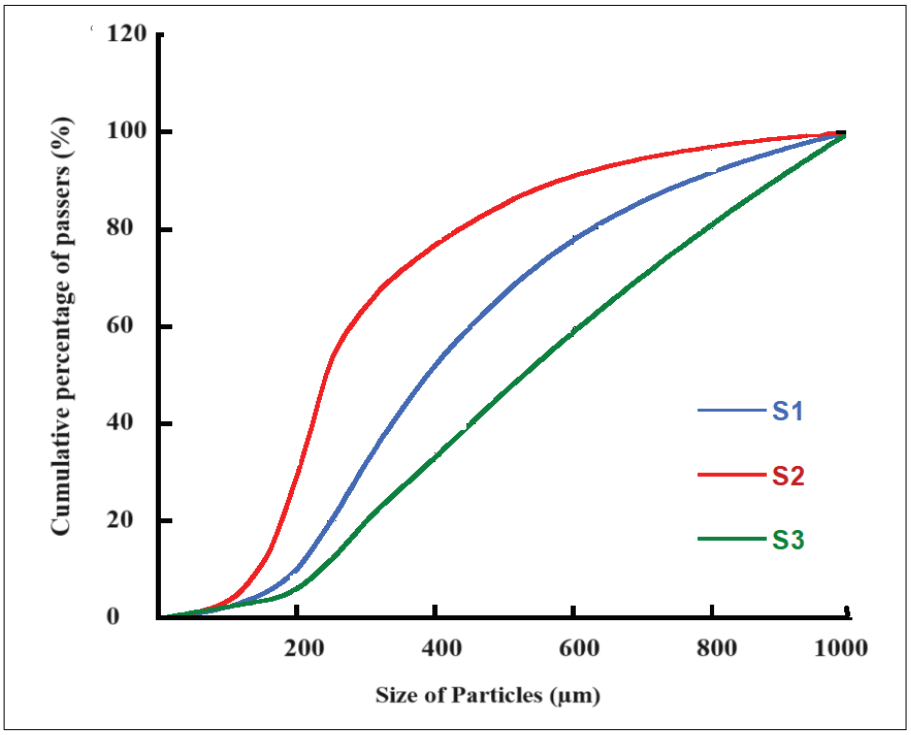

Fig. 11. S_1, S_2 and S_3 granulometric distribution

Table 3. Granulometric parameters and uniformity coefficients for S_1, S_2, and S_3 samples

Parameters	d_{10} (µm)	d_{50} (µm)	d_{60} (µm)	d_{90} (µm)	CU
S_1	200	390	440	840	2.2
S_2	150	240	275	650	1.8
S_3	230	530	625	910	2.7

The main granulometric parameters and the coefficient of uniformity (CU) of the three sand samples were determined based on the granulometric analysis curves. These data are presented in Table 3. Among the three sand samples, S_1 and S_3 have CU values that exceed the range recommended for sand filtration. The S_2 sample falls within the recommended range with a CU value of 1.8. This sand is more homogeneous and more suitable for filtration [2]. So, it will be used for our filtration tests.

The complete granulometric analysis curve for GOM is shown in Figure 12. We extract the gravel sample's main granulometric parameters and its uniformity coefficient from this granulometric curve. The GOM's main granulometric parameters and coefficient of uniformity are shown in Table 4.

3.2.2.Manganese (II) removal tests

The results of manganese (II) removal tests as a function of aeration time and pH are shown in Figure 13. For filtration, the sand used is suitable S_2, and the gravel was GOM.

Manganese removal corresponds to Mn (II) oxidation by atmospheric oxygen. This oxidation is followed by its respective precipitation on the filter as manganese oxide MnO_2. The manganese oxidation reaction is written [32-34].

$$2Mn^{2+} + O_2 + 2H_2O \rightarrow 2MnO_2\downarrow + 4H^+ \quad \text{(Eq. 5)}$$

The aeration-filtration process allows a removal rate of manganese, after 2 hours of aeration, of 74.8% at pH 6, 79.3% at pH 7, and 84.5% at pH 8. It should be noted that at pH 8 and for one hour of

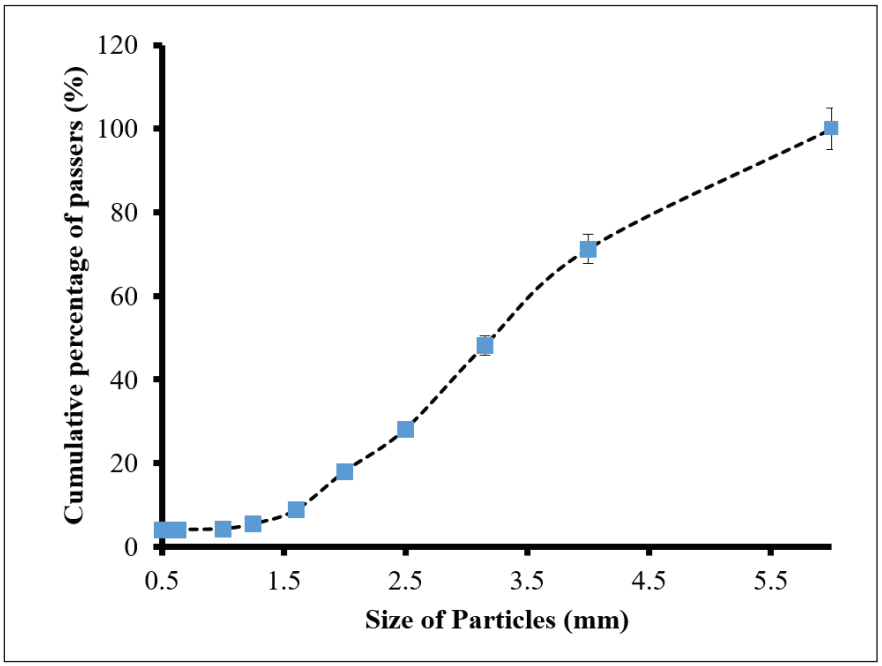

Fig. 12. GOM granulometric distribution

Table 4. The GOM's main granulometric parameters and coefficient of uniformity

Parameters	d_{10} (mm)	d_{50} (mm)	d_{60} (mm)	d_{90} (mm)	CU
GOM	1.65	3.2	3.5	5.25	2.1

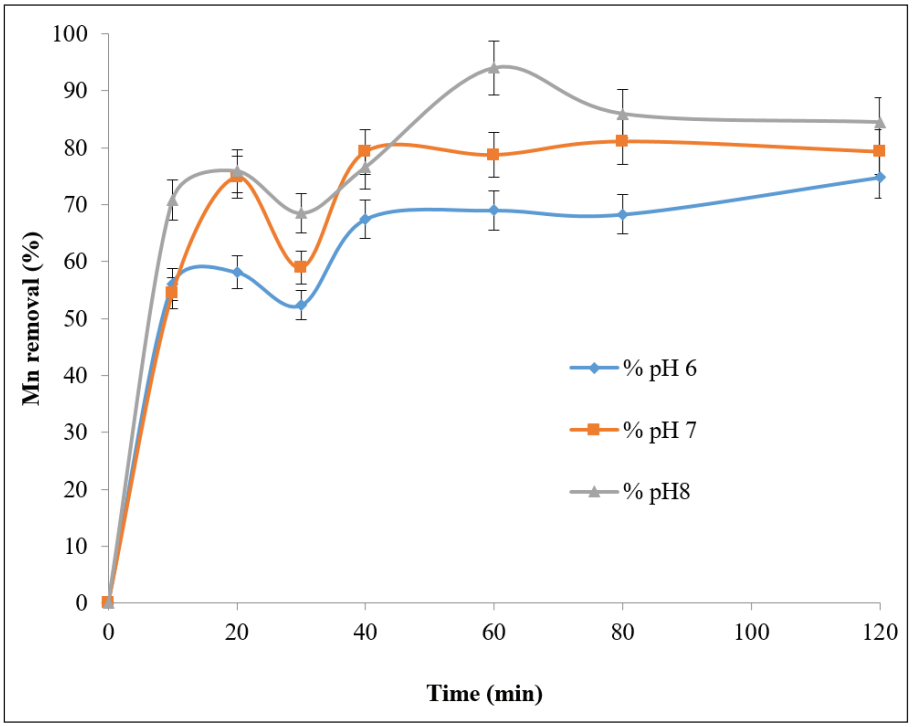

Fig. 13. Evolution of manganese removal rate during aeration-filtration at different pH values

aeration, we obtained a removal rate of 95%. This value decreased and stabilized at 84.5% after 2 hours of aeration. The removal of manganese is highly dependent on the pH of the water [35]. Also, manganese removal increases with pH. Several studies have concluded that manganese cannot be removed with simple aeration using atmospheric oxygen [17]. As a result of successive filtrations on the same sand filter, manganese can precipitate or adsorb onto the manganese oxide formed [2], which justifies the high removal rates. In this study, manganese removal rates are similar to those in the literature. Also, Lanciné et al. used aeration followed by sand filtration to remove iron and manganese from borehole water in rural areas. In this process, 71% of manganese was removed after 1 hour of air aeration [2]. Cheng et al. used aeration, a manganese sand filter, and ultrafiltration for manganese removal from water. By using this process, manganese can be removed from water by 90% [36]. Jeż-Walkowiak and colleagues researched the filtration process on the pilot scale using three different filtration materials. In all of the research cycles, they demonstrated high efficiency in manganese removal and the highest stability of effects with the auto-activated bed (100%); Gabon manganese ore was characterized by high efficiency (90%) in removing manganese from filtrated water; silica sand was represented in the beginning by the lowest Mn removal efficiency (20%) but was observed to increase with time [37]. El-Naggar obtained similar results when he investigated the removal of Mn through the filtration of different types of sand at different depths and during filtration. According to this author, the best results were obtained at a filter material depth of 90 cm, producing a manganese removal rate of 100% [38]. Using aeration and coagulation-flocculation, Ntakiyiruta et al. demonstrated the possibility of removing manganese ions with an efficiency of over 90.34 percent [17]. The removal rates obtained by this method are also comparable to those obtained by biological treatment. Casalini et al. proposed a biological manganese removal process that achieved a 95% removal rate at the filter outlet [39]. The researchers showed that manganese (II) can also be removed from water by nanotechnology processes [40]. El Shahawy et al. removed Mn (II) ions from wastewater using an AgNPs/GO/chitosan nanocomposite material. Their study achieved a high removal rate of 97.9% [40].

4. Conclusion

As part of the present work, we have developed an electrochemical sensor for determining manganese (II) in the presence of the ligand 2-(5'-Bromo-2'-pyridylazo)-5-diethylaminophenol (5-Br-PADAP) on a carbon paste electrode. By optimizing the analytical parameters with cathodic stripping voltammetry (CSV), the sensor has determined the manganese content of water samples taken from wells and boreholes. The manganese content of the water analyzed ranged from 4.36×10^{-3} to 1.738 $mg.L^{-1}$. Therefore, treating water with manganese levels exceeding the WHO standard is necessary. An investigation was conducted in the laboratory to develop a low-cost process for removing manganese from boreholes and well waters, particularly by aeration and filtration. Based on air-oxygen oxidation and then filtration on sand and gravel, the process can be used in rural, suburban, and family environments without strong oxidants, which are generally toxic chemicals. The manganese removal efficiencies achieved in this study (74.8% to 84.5% for two h of aeration, 97% at pH 8, and for one h of aeration) demonstrate the interest in using this process in rural areas, particularly in developing countries with low incomes.

5. Acknowledgment

The authors thanks to the Department of Chemistry, Faculty of Science and Technology, Abdou Moumouni University, Niamey, Niger. The financial support of the International Science Programme [ISP], Uppsala, Sweden is gratefully acknowledged.

6. References

[1] J. Rodier, B. Legube, N. Merlet, B. Regis, Natural waters, wastewater, seawater: Water analysis (L'analyse de l'eau), Dunod, 10th edition, 2016. https://www.dunod.com/sciences-techniques/analyse-eau-eaux-naturelles-eaux-residuaires-eau-mer-0

[2] G.D. Lanciné, A.J. Touchard, K. Bamory, K. Fernand, K. Kouadio, S. Issiaka, Removal of iron and manganese by aeration-filtration of borehole water in rural areas in developing countries, the case of the Tassialé region (southern Côte d'Ivoire), Eur. J. Sci. Res., 19 (2008) 558-567. http://www.eurojournals.com/ejsr.htm

[3] A.A. Mahamane, G. Boubié, Physico-chemical characterizations of groundwater in the locality of Yamtenga (Burkina Faso), Int. J. Biol. Chem. Sci., 9 (2015) 517-533. https://doi.org/10.4314/ijbcs.v9i1.44

[4] R. Mogwasi, M. Eric, N. Obed, Inductively coupled plasma-mass spectrometry versus flame atomic absorption spectrophotometry for the analysis of Fe, Cu, Zn, Mn, and Cr in medicinal plants: a comparison study, Adv. Transl. Med., 2 (2023) 1-15. https://doi.org/10.55976/atm.220231321-15

[5] R.D. Crapnell, E.B. Craig, Electroanalytical overview: The determination of manganese, Sens. Actuators Rep., 4 (2022) 100110. https://doi.org/10.1016/j.snr.2022.100110

[6] S. Sima, S. Cinti, Anodic and cathodic stripping voltammetry for metals sensing, Electrochem., 17 (2023) 55-72. https://doi.org/10.1039/BK9781839169366-00055

[7] Y. Yang, Y. Huang, H. Luo, J. Zao, J. Bi, G. Wu, Ion interference and elimination in electrochemical detection of heavy metals using anodic stripping voltammetry, J. Electrochem. Soc., 170 (2023) 057507. https://doi.org/10.1149/1945-7111/acd1ba

[8] I. Dominguez, M.C. Jesus, D.V. Ignacio, D.M. Juan, S. Radka, S. Petr, S. Vitezslav, Ś. Mateusz, R. M. Ignacio, Electrochemical lossy mode resonance for detection of manganese ions, Sens. Actuators B Chem., 394 (2023) 134446. https://doi.org/10.1016/j.snb.2023.134446

[9] G. Ringgit, S. Shafiquzzaman, S. Surayani L. Mohammad, Synthesized f-MWCNTs/CS/PB for determination of manganese (Mn^{2+}) in drinking water, Monatsh. Chem., 154 (2023) 191-203. https://doi.org/10.1007/s00706-022-03026-3

[10] E. Boselli, Z. Wu, A. Friedman, C.B. Henn, L. Papautsky, Validation of electrochemical sensor for determination of manganese in drinking water, Environ. Sci. Technol., 55 (2021) 7501-7509. https://doi.org/10.1021/acs.est.0c05929

[11] C. Mariame, Y.N. Alfred, B. Drissa, G.M. El Amine, Y.M. Issa, E.R. Mama, Assessment of dissolved manganese (II) pollution in river water by differential pulse cathodic stripping voltammetry: A case study of River Boubo, Côte d'Ivoire, Afr. J. Pure Appl. Chem., 7 (2013) 318-324. https://doi.org/10.5897/AJPAC2013.0516

[12] H.S. El-Desoky, M.I. Iqbal, M.G. Mohamed, Stripping voltammetry method for determination of manganese as complex with oxine at the carbon paste electrode with and without modification with montmorillonite clay, J. Solid State Electrochem., 17 (2013) 3153-3167. https://doi.org/10.1007/s10008-013-2204-2

[13] E. M Ghoneim, Simultaneous determination of Mn (II), Cu (II) and Fe (III) as 2-(5′-bromo-2′-pyridylazo)-5-diethylaminophenol complexes by adsorptive cathodic stripping voltammetry at a carbon paste electrode, Talanta, 82 (2010) 646-652. https://doi.org/10.1016/j.talanta.2010.05.025

[14] A.A. Mahamane, C. Despas, R. Adamou, A. Walcarius, Carbon paste electrode modified with 5-Br-PADAP as a new electrochemical sensor for the detection of inorganic mercury (II), J. Mater. Environ. Sci., 13 (2022) 54-69. http://www.jmaterenvironsci.com

[15] T. Chu, M. Cheng, S. Hou, Y. Yang, Modified graphite paper treated by anionic intercalation

for manganese removal via electrochemical deposition in water treatment, J. Ind. Eng. Chem., 120 (2023) 504-513.https://doi.org/10.1016/j.jiec.2023.01.002

[16] S.M. Safwat, N.Y. Mohamed, M.M. El-Seddik, Performance evaluation and life cycle assessment of electrocoagulation process for manganese removal from wastewater using titanium electrodes. J. Environ. Manage., 328 (2023)116967. https://doi.org/10.1016/j.jenvman.2022.116967

[17] P.Ntakiyiruta,P.C.Mpawenayo,D.Rucakumugufi, P. Bigumandondera, T. Ndikumana, J.L. Vasel, Removal of iron and manganese by aeration and coagulation-flocculation in borehole water from the town of Rumonge (Burundi), J. Mater. Environ. Sci., 14 (2023) 141-152. http://www.jmaterenvironsci.com

[18] K.L. Dishman, Sieving in particle size analysis, Encyclopedia of Analytical Chemistry application, theory, and instrumentation, Wiley publisher, 2006. https://doi.org/10.1002/9780470027318.a1514

[19] P. Charles, Catalytic removal of iron and manganese for the production of drinking water, water technologies drinking water supply, Suez Environnement, 2006. https://www.eurochlore.fr/wp-content/uploads/2016/12/Rapport_06AEP07.pdf

[20] M. Gharous, L. Bounab, F.J. Pereira, M. Choukairi, R. López, A.J. Aller, Electrochemical kinetics and detection of paracetamol by stevensite-modified carbon paste electrode in biological fluids and pharmaceutical formulations, Int. J. Mol. Sci., 24 (2023) 11269. https://doi.org/10.3390/ijms241411269

[21] A.A. Mahamane, B. Guel, P.L. Fabre, Electrochemical behavior of iron (II) at a nafion-1, 10-phenanthroline-modified carbon paste electrode: Assessing the correlation between Preconcentration potential, surface morphology, and impedance measurements, Challenge Adv. Chem. Sci., 2 (2021) 52–71.https://doi.org/10.9734/bpi/cacs/v2/2419F

[22] S. A Leau, C. Lete, C. Matei, S. Lupu, Electrochemical sensing platform based on metal nanoparticles for epinephrine and serotonin, Biosens., 13 (2023) 781. https://doi.org/10.3390/bios13080781

[23] C.M. Welch, C.E. Banks, Š. Komorsky-Lovrić, R.G. Compton, Electroanalysis of trace manganese via cathodic stripping voltammetry: exploration of edge plane pyrolytic graphite electrodes for environmental analysis, Croat. Chem. Acta, 79 (2006) 27–32. https://core.ac.uk/download/pdf/14377079.pdf

[24] B. Rezaei, M. Ghiaci, M.E. Sedaghat, A selective modified bentonite–porphyrin carbon paste electrode for determination of Mn(II) by using anodic stripping voltammetry, Sens. Actuators B, 131 (2008) 439–447. https://doi.org/10.1016/j.snb.2007.12.017

[25] S. B. Khoo, M. K. Soh, Q. Cai, M. R. Khan, S. X. Guo, Differential pulse cathodic stripping voltammetric determination of manganese (II) and manganese (VII) at the 1-(2-pyridylazo)-2-naphthol-modified carbon paste electrode, Electroanalysis, 9 (1997) 45–51. https://doi.org/10.1002/elan.1140090111

[26] M. Aghaie, M. Giahi, M. Zawari, Manganese(II) ion-selective membrane electrode based on N-(2-picolinamido ethyl)-picolinamide as neutral carrier, Bull. Korean Chem. Soc., 31 (2010) 2980–2984. https://doi.org/10.5012/bkcs.2010.31.10.2980

[27] S. Sharma, A. Jaiswal, K.N. Uttam, Synthesis of sensitive and robust lignin capped silver nanoparticles for the determination of cobalt(II), chromium(III), and manganese(II) ions by colorimetry and manganese(II) ions by surface-enhanced raman scattering (SERS) in aqueous media, Anal. Lett., 54 (2021) 2051-2069. https://doi.org/10.1080/00032719.2020.1837855

[28] J. Rakhtshah, M. Dehghani Mobarake, Simultaneously speciation and determination

of manganese (II) and (VII) ions in water, food, and vegetable samples based on immobilization of N-acetylcysteine on multi-walled carbon nanotubes, Food Chem., 389 (2022) 133124. https://doi.org/10.1016/j.foodchem.2022.133124

[29] A.Khaligh,H.Z.Mousavi,A.Rashidi, Ultrasound assisted-dispersive-micro-solid phase extraction based on bulky amino bimodal mesoporous silica nanoparticles for speciation of trace manganese (II)/(VII) ions in water samples, Microchem. J., 124 (2016) 637–645. https://doi.org/10.1016/j.microc.2015.10.008

[30] D. Citak, M. Tuzen, M. Soylak, Speciation of Mn(II), Mn(VII) and total manganese in water and food samples by coprecipitation–atomic absorption spectrometry combination, J. Hazard. Mater., 173 (2010) 773–777.https://doi.org/10.1016/j.jhazmat.2009.09.004

[31] S. Golkhah, H. Zavvar Mousavi, Removal of Pb (II) and Cu (II) Ions from aqueous solutions by cadmium sulfide Nanoparticles, Int. J. Nanosci. Nanotechnol., 13 (2017) 105-117. https://www.ijnnonline.net/article_25609.html

[32] S. Kouzbour, N. El Azher, B. Gourich, F. Gros, C. Vial, Y. Stiriba, Removal of manganese (II) from drinking water by aeration process using an airlift reactor, J. Water Process. Eng., 16 (2017) 233–239.https://doi.org/10.1016/j.jwpe.2017.01.010

[33] L. Schamphelaire, R. Korneel, N. Boon, W. Verstraete, P. Boekx, Minireview: The potential of enhanced manganese redox cycling for sediment oxidation, Geomicrobiol. J., 24 (2007) 547-558.https://doi.org/10.1080/01490450701670137

[34] S. Jerroumi, M. Amarine, B. Gourich, Technological trends in manganese removal from groundwater: A review, J. Water Process. Eng., 56 (2023) 104365. https://doi.org/10.1016/j.jwpe.2023.104365

[35] K. Fialova, M. Motlochova, L. Cermakova, K. Novotna, J. Bacova, T. Rousar, M. Pivokonsky, Removal of manganese by adsorption onto newly synthesized TiO2-based adsorbent during drinking water treatment, Environ. Tech., 44 (2023) 1322-1333. https://doi.org/10.1080/09593330.2021.2000042

[36] L.H. Cheng, Z.Z. Xiong, S. Cai, D.W. Li, X.H. Xu, Aeration-manganese sand filter-ultrafiltration to remove iron and manganese from water: Oxidation effect and fouling behavior of manganese sand coated film, J. Water Process. Eng., 38 (2020) 10162. https://doi.org/10.1016/j.jwpe.2020.101621

[37] J.J. Walkowiak, Z. Dymaczewski, A.S. Janiaczyk, A.B. Nowicka, M. Szybowicz, Efficiency of Mn removal of different filtration materials for groundwater treatment linking chemical and physical properties, Water, 9 (2017) 498. https://doi.org/10.3390/w9070498

[38] H.M. El-Naggar, Development of low-cost technology for the removal of iron and manganese from groundwater in Siwa Oasis, J. Egypt. Public Health Assoc., 85 (2010). 169-188. https://pubmed.ncbi.nlm.nih.gov/21244816/

[39] L.C. Casalini, A. Piazza, F. Masotti, V. A. Pacini, G. Sanguinetti, J. Ottado, N. Gottig, Manganese removal efficiencies and bacterial community profiles in non-bioaugmented and in bioaugmented sand filters exposed to different temperatures, J. Water Process. Eng., 36 (2020) 101261 .https://doi.org/10.1016/j.jwpe.2020.101261

[40] A. El Shahawy, M.F. Mubarak, M. El Shafie, H.M. Abdulla, Adsorption of Mn (II) ions from wastewater using an AgNPs/GO/chitosan nanocomposite material, RSC Adv., 12 (2022) 29385-29398. https://doi.org/10.1039/D2RA04693H